Predicting Transportation Carbon Emission with Urban Big Data

Predicting Transportation Carbon Emission with Urban Big Data

Xiangyong Lu, Kaoru Ota, *Member, IEEE,* Mianxiong Dong, *Member, IEEE,* Chen Yu, *Member, IEEE,* and Hai Jin, *Senior Member, IEEE*

Abstract—Transportation carbon emission is a significant contributor to the increase of greenhouse gases, which directly threatens the change of climate and human health. Under the pressure of the environment, it is very important to master the information of transportation carbon emission in real time. In the traditional way, we get the information of the transportation carbon emission by calculating the combustion of fossil fuel in the transportation sector. However, it is very difficult to obtain the real-time and accurate fossil fuel combustion in the transportation field. In this paper, we predict the real-time and fine-grained transportation carbon emission information in the whole city, based on the spatio-temporal datasets we observed in the city, that is taxi GPS data, transportation carbon emission data, road networks, points of interests (*POI*s) and meteorological data. We propose a three-layer perceptron neural network (3-$layerPNN$) to learn the characteristics of collected data and infer the transportation carbon emission. We evaluate our method with extensive experiments based on five real data sources obtained in Zhuhai, China. The results show that our method has advantages over the well-known three machine learning methods (Gaussian Naive Bayes, Linear Regression, Logistic Regression) and two deep learning methods (Stacked Denoising Autoencoder, Deep Belief Networks).

Index Terms—Transportation carbon emission, urban big data, multilayer perceptron neural network, real-time prediction.

1 Introduction

Transportation carbon emission is the main source of greenhouse gases (*GHG*). Between 2000 and 2010, carbon emission from transportation sector contributed about 11% to the total annual anthropogenic *GHG* emissions increase. The Intergovernmental Panel on Climate Change (*IPCC*) estimates that in the absence of effective emission reduction policies, the baseline global *GHG* emissions will increase anywhere from 25 to 90 percent between the years 2000 and 2030. With the increases of global *GHG* emissions, the average global temperatures will continue to rise. The increases in global temperatures will most likely cause our planet's climate change in ways that will have significant long-term effects on human health and the environment. Given the importance of devising efficient emission reduction strategies, it is essential for policy makers to obtain the real-time and fine-grained information about carbon emission according to local conditions.

Unfortunately, even in the same city, transportation carbon emission differs in different places and relys on multiple factors, such as road traffic, human mobility and structure of road network. For instance, in Zhuhai, we divide the city into disjoint and uniform grids, as depicted in Figure 1(a). It is clear that each grid has different spatial distribution of the road networks and *POI*s, even though they border each other, as shown in Figure 1(b). The green line segments stand for road segments, the blue dots represent the *POI*. Figure 2(a) clearly exposes that the transportation carbon emission of different grids is diverse at 5pm on 9/26/2015, even if they are closed to each other. For example, the grid $G26$ and grid $G37$ are adjacent, the transportation carbon emission of them is very different. Figure 2(b) further reveals that carbon emission from transportation in an area changes with time of day. The adjacent areas have different time variation curves, such as $G18$ and $G26$. These results indicate that the transportation carbon emission of one region close correlate with its spatial and temporal characteristics.

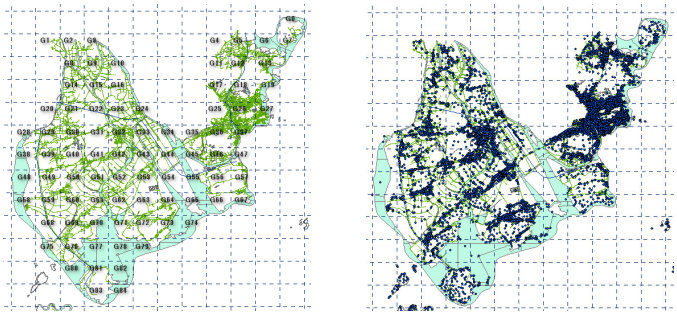

(a) Girds in Zhuhai city (b) The density of road networks and *POI*

Fig. 1. The spatial geographical information of Zhuhai city

In this paper, we take advantage of the excellent feature learning ability of multi-layer network architectures. We propose a three-layer perceptron neural network (3-

- *X. Lu, C. Yu and H. Jin are with the Serviecs Computing Technology and System Lab, Big Data Technology and System Lab, Cluster and Grid Computing Lab, School of Computer Science and Technology, Huazhong University of Science and Technology, Wuhan, 430074, China. X. Lu is also an Visiting Student with the Department of Information and Electronic Engineering, Muroran Institute of Technology, Muroran, Hokkaido, Japan. C. Yu is the corresponding author.*
  E-mail: m201572848@hust.edu.cn,16061102@mmm.muroran-it.ac.jp; yuchen@hust.edu.cn; hJin@hust.edu.cn
- *K. Ota, M. Dong are with the Department of Information and Electronic Engineering, Muroran Institute of Technology, Muroran, Hokkaido, Japan.*
  E-mail: ota@csse.muroran-it.ac.jp; mx.dong@csse.muroran-it.ac.jp

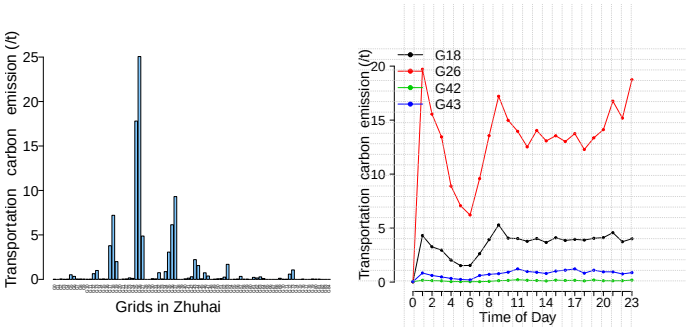

(a) Transportation carbon emissions of all girds at 5pm on 9/26/2015

(b) The time variation curves of transportation carbon emission on 9/26/2015

Fig. 2. The transportation carbon emission between difference grids

$layerPNN$) model to infer the real-time and fine-grained transportation carbon emission in each region, based on the heterogeneous spatio-temporal data sources in the city, such as meteorology, road traffic, human mobility, structure of road networks and *POI*s. Although, in previous studies, the environment scientists and governmental agencies have proposed some greenhouse gas emission calculation methods and models, such as top-down and bottom-up models [1]. Carbon emission from transportation is usual estimated by separating from the total urban carbon emission from fossil fuel combustion. It is calculated as a simple product of the following factors: fuel consumption, the carbon coefficient of a particular fuel and the percent of fuel that is combusted [2]. However, different degrees of uncertainty will be introduced, when the fossil fuel combustion is measured in different ways. The carbon emission coefficients vary with region and country. Besides, these methods and models often work with limited sets of factors and empirical parameters, which are often not applicable to other regions with different environments. In addition, it is difficult to obtain the real time fossil fuel combustion in the transportation field.

Due to the considerable amount and diversity of the raw urban data, it is not advisable to use them directly to train our model. For achieving excellent prediction performance, we firstly extract five kinds of feature datasets ($F_t, F_{Mo}, F_p, F_{RN}, F_{Me}$) based on the relationships between the datasets and transportation carbon emission. Moreover, combined with the selected features, we train our model to learn the neural network parameters and use the trained model to predict the future transportation carbon emission. Furthermore, we evaluate our method using the real world datasets.

Our work presents a multilayer neural network prediction model to infer the regional transportation carbon emission, leveraging the multiple urban data. The challenges of our approach lie in three aspects. The first is to identify the efficient features from the heterogeneous data sources. The second is the calculation of transportation carbon emission in each area based on the "top-down" method proposed by the *IPCC*. The Third is how to construct the multilayer neural network to get the better performance. The main contributions of this paper include:

1. We devise a multilayer perceptron neural network prediction model, which learns the model parameters leveraging diverse feature datasets. This prediction model could accurately predict the regional transportation carbon emission in the future period of time.

2. We identify five kinds of feature datasets ($F_t, F_{Mo}, F_p, F_{RN}, F_{Me}$), based on the multiple urban data. These feature datasets can not only be applied to our prediction model, but also could be used in the prediction of other automobile exhaust emissions.

3. We evaluate our method based on the multiple datasets in Zhuhai city, that is meteorological data, road networks, *POI*s, transportation carbon emission data and the *GPS* trajectories generated by over 3,000 taxicabs in Zhuhai city from August 1st to October 14th, 2015. And we justify the advantages of our method over the other three machine learning algorithms and two deep learning algorithms.

The rest of the paper is organized as follows. We first present the related work in section 2. Then we formally make some preliminary definitions and describe the framework of our system in section 3. We introduce the feature extraction in section 4. Feature learning and inference are discussed in section 5. Experimental evaluation is shown in section 6. Finally, we conclude our work in section 7.

2 Related Work

2.1 Greenhouse Gases Estimation and Prediction

Greenhouse gases provide us with a hospitable living environment by trapping some of the sun's natural heat. The main sources of *GHG*s consist of the electricity production, transportation and industry. With the advancement of urbanization and industrialization, *GHG*s concentrations in the atmosphere continue to increase. Under this background, researches on the statistics and projections of *GHG*s attract many scientists and research institutions around the world. There are two major approaches to estimate the *GHG*s emissions, that are "top-down" and "bottom-up" models proposed by the *IPCC* [1]. The "top-down" approach firstly calculates the total carbon emission from the total fuel consumption in the city. The total carbon emission then is apportioned to each economic sector, such as transportation sector. As carbon emission varies in locations non-linearly, this model would not capture the accurate estimate of the carbon emission according to local conditions. The "bottom-up" approach directly calculates the fuel consumption from each economic sector. Then the amount of carbon emission is calculated according to the carbon emission parameters of the fuel.

However, there are many uncertainties in the calculation of these two models. The uncertainties are mainly from the empirical assumptions and the uncertainty in the primary data: fuel consumption, carbon content, and oxidation factors [3]. When the total carbon emission is allocated to the individual sectors, additional uncertainties are always being introduced. Compared with the previous work in this area, in this paper we calculate the exact amount of carbon emission from the transportation sector, utilizing the multiple local data sources to increase the reliability of input data. What's more, the increasing numbers of sensors in the city provide us with rich source data. A wide variety of

urban data will not only help us to understand the dynamics of the city, but also help us to optimize the urban structure.

2.2 Urban Computing

With the increasing number of city data, researches on urban computing become more attractive. Urban computing is described in detail in paper [4]. Zheng [5] proposed a semi-supervised learning approach based on a co-training framework to infer the urban air quality, based on the air quality data and a variety of data sources. Karamshuk [6] used the supervised regression model and supervised learning model to optimize the placement of the retail stores. He extracted the features by studying the predictive power of various features on the popularity of retail stores based on the dataset collected from Foursquare in New York. Nevertheless, Zhang [7] combined the supervised and unsupervised machine learning techniques to identify the traffic of zero-day applications in a network. Compared with their interesting and influential work, in this paper we devise a multilayer perceptron neural network model to predict the transportation carbon emission, leveraging multiple urban data sources. The biggest difference between Zheng's research and mine is that the characteristics of the training methods are different. He divides the feature datasets into two parts, and uses them to train different models, However we utilize the all feature datasets to train a 3-$layer PNN$ model. Compared with Karamshuk's research, our training datasets are much more diverse.

Yang [8] modeled the spatial and temporal activity preference separately and then used a principle way to combine them for the preference inference. Fan [9] proposed a predicting-by-clustering framework to predict crowd behavior at a citywide level based on human mobility big data. Shimosaka [10] proposed a low-rank bilinear Poisson regression model to predict the urban dynamics, utilizing the one year's worth of mobility records. Li [11] proposed a smart city infrastructure to serve people, based on the multi-sensors data. Sun [12] promoted the concept of smart and connected communities, based on the Internet of Things Technologies and big data analytics. Yang [13] proposed a Wifi-based, real-time monitoring of a carbon monoxide system for application in the construction industry. Wang [14] provided an overview of water cyber-physical systems for sustainability. Compared to their studies, the present paper predict the transportation carbon emission leveraging the spatial-temporal urban data, such as meteorology, road traffic, structure of road networks and POIs. The training datasets are different between their work and mine. we extend the application of multi-layer neural networks to the field of carbon emission analytics.

2.3 Traffic optimization

With the increasing deployment of sensors on the roads and vehicles, it will help us get more urban traffic data. And with the help of these data, a series of researches on city traffic have been done recently, including traffic forecasting, congestion management, vehicle distribution and vehicle routing. Abadi [15] implemented an optimization methodology to predict the flows of a traffic network in San Fransico, based on the real-time and estimated traffic data. Wang [16] presented an interactive system for visual analysis of urban traffic congestion, based on *GPS* trajectories. Zhang [17] proposed a data-driven system to sense the refueling behavior and citywide petrol consumption in real time, based on a trajectory dataset, *POI* dataset and road network dataset. Chan [18] proposed an intelligent particle swarm optimization algorithm to develop short-term traffic flow predictors, based on the dataset captured by on-road sensors. Chen [19] adopted the regression-and-ranking methodologies to predict the potential bike trip demand, utilizing the highly variant urban open data. Compared with them, we concentrate on inferring the transportation carbon emission, mainly utilizing the traffic related data. Our work can be seen as an extension of traffic to the environment.

3 Overview

3.1 Preliminary

Definition 1: *Transportation carbon emission.* The transportation carbon emission is a measure of the total amount of carbon dioxide emissions emitted through the combustion of fossil fuels, which are directly and indirectly caused by the traffic. The *IPCC* guidelines for national greenhouse gas inventories [1] gives two calculation methods, respectively, "top-down" and "bottom-up" approach. The "top-down" approach is formulated in Equation 1 as follows:

$$W = \sum_{i \in N} \sum_{j \in N} K_{i,j} \cdot n_{i,j} \cdot s_{i,j} \cdot e_{i,j}, \tag{1}$$

where W represents the total amount of transportation carbon emission. $K_{i,j}$ represents the carbon dioxide emission coefficient of j type of fuel consumed by i vehicle type. i is a kind of vehicle types. j is a type of fuel. n is the number of vehicles. s represents the transport mileage of vehicles. e stands for the average intensity of consumption per unit mileage.

The "bottom-up" approach is formulated in Equation 2 as follows:

$$W = \sum_{j \in N} (K_j \cdot E_j - M) \cdot \varphi_j \cdot \frac{44}{12}, \tag{2}$$

where K_j represents the carbon dioxide emission coefficient of j type of fuel. E_j represents the amount of carbon emission of j type of fuel. M represents the amount of carbon fixation. φ_j stands for the share of fuel oxidation.

Definition 2: *Trajectory.* A spatial trajectory T is a sequence of *GPS* points that are time-ordered spatial points, T:$p_1 \rightarrow p_2 \rightarrow ... \rightarrow p_n$. Each GPS point p_i consists of a longitude, a latitude and a timestamp.

Definition 3: *POI.* A *POI* is a specific point location in the physical world, consisting of a name, category, longitude, latitude. It is a place where a lot of people can find interesting and useful.

Definition 4: *Road network.* A road network RN is a network structure formed by road segments. Each road segment r connects each others and has different functions and locations.

Definition 5: *Grid.* We divide a city into disjoint and uniform grids (e.g.,$5km \times 5km$ in the experiments) as illustrated in Figure 1(a). Each grid g has its carbon emission $g.W$, which

stands for the total amount of carbon emission in the grid g. The coordinate of each grid center is used as the coordinate of the grid. We assuming the meteorological of the city is uniform in one day.

Definition 6: *Neuron.* A multiple-input neuron is shown in Figure 3. The individual inputs $P_1, P_2, ..., P_R$ are each weighted by corresponding elements $w_{11}, w_{12}, ..., w_{1R}$. The b is a bias. The f represents the activation function. The a represents the output of the neuron. The neuron can be formulated as the Equation 3.

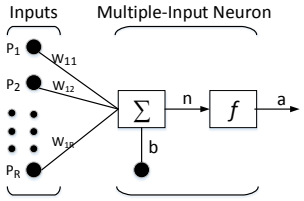

Fig. 3. Multiple-Input Neuron

$$a = f(n) = f(\sum_{i=0}^{R}(P_i \cdot W_{1i}) + b), \quad R \in N \tag{3}$$

3.2 Framework

Our aim is to train a multilayer perceptron neural network to infer the future information of transportation carbon emission throughout the city. Primarily, we collect and filter the relevant source data according to the prior knowledge. Additionally, we preprocess the raw data and extract the features that are closely related to the transportation carbon emission. For obtaining the labeled data, we calculate the amount of transportation carbon emission in each gird based on the processed trajectory datasets. Furthermore, using the extracted features and labeled data, we train the proposed 3-$layerPNN$ model to learn the model parameters. Accordingly, based on the trained neural network model, we predict the transportation carbon emission of each grid during the future period of time. Our framework consists of four main parts, as shown in Figure 4.

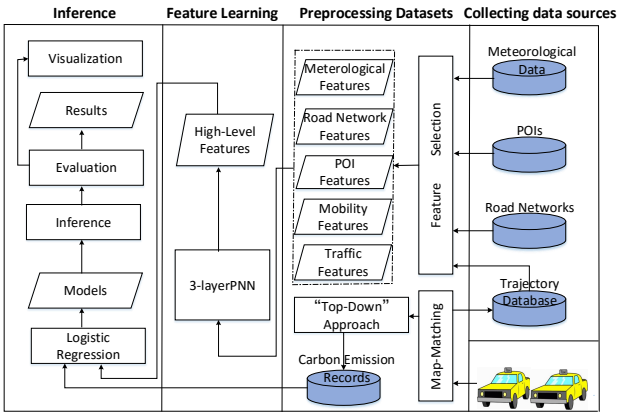

Fig. 4. Framework of our system

Collecting data sources: In this part, we select four real-world datasets, respectively, the taxi trajectories, road networks, *POI*s and meteorological data. We get the spatial trajectories generated by over 3,000 taxicabs in Zhuhai city during a period of nearly three months. The *POI* dataset consists of nearly 40,000 *POI*s in this city. The road network dataset contains about 3,0277 road segments.

Preprocessing datasets: Each trajectory is extracted from the raw trajectory datasets and mapped onto the road networks to improve the quality of the data. Then we utilize the "top-down" approach to calculate the amount of transportation carbon emission of each grid using the cleaned trajectory data. Accordingly, we obtain the transportation carbon emission dataset. Then we extract the diverse spatio-temporal features that are closely related to transportation carbon emission, based on the correlation and the effect on the prediction accuracy after the fusion with other features. In the process of extraction, we try to keep the original attributes of the source data. Finally, prior to training, we regularize these feature datasets. Detailed in section 4.

Feature learning: We feed the extracted features into our 3-$layerPNN$ model to train the neural network structure and optimize the learning parameters. The transportation carbon emission data is used as the labeled data for the supervised learning. Detailed in section 5.

Inference: Based on the trained network structure and the learning parameters, we use the logistic regression method to infer the future transportation carbon emission for each grid once every hour. See section 5 for details.

Problem statement

Given a collection of grids $G = \{g_1, g_2, ..., g_n\}$, where $g_i.W$ is the carbon emission of the grid g_i, a road network RN crossing G, a *POI* located in G, a trajectory dataset T passing G, and a record of meteorological data in G, we intend to infer the $g_i.W'$ in the future.

4 Feature Extraction

4.1 Traffic Features: F_T

The traffic features are the main characteristics to infer the transportation carbon emission. Usually, the gasoline-fueled vehicles have three operating mode conditions, that is cold start, hot start, and hot stabilized. Under different condition, the vehicles have significantly different emission rates. The vehicle speed and travel length are also the important features in the study of transportation carbon emission. Accordingly, we select five relative features for each grid, that is the number of start operations, expectation of speeds , standard deviation of speeds, the number of vehicles and the travel length. Figure 5 shows the correlation matrix between the first four features and transportation carbon emission. These features are extracted from the *GPS* trajectories generated by vehicles traversing the grid in the past hour.

Number of start operations: $NumSta$**.** Given a spatial trajectory of a vehicle, we retrieve all the track points that fall in the affecting region of each grid ($p.l \in g.R$, $p.l$ represents the location of the point p). The points contained in the trajectory are strictly increasing in time. We check the two adjacent points. If the speed of the former point p_i equals to zero, meanwhile the speed of the later point p_{i+1} is not

equal to zero, we believe that there is a start event. We count the start action times *NumSta* according to Equation 4.

$$Sat = Sat + 1, \qquad p_i.v = 0, p_{i+1}.v \neq 0, \tag{4}$$

where p_i, p_{i+1} fall in the same grid g.

Expectation of speeds: $E(v)$**.** We also retrieve the track points of the trajectories that fall in the affecting region of each grid. As the sampled data of the GPS device is discrete, we use the expectation of speeds to represent all the speeds of passing vehicles in $g.R$. We first design a formula to calculate the distance between two consecutive points, as Equation 5. We then calculate the total driving distance and the traveling time. Finally, we calculate the expectation of speeds according to Equation 6.

$$Dist(p_i, p_{i+1}) = \frac{p_i.v + p_{i+1}.v}{2} \cdot |p_{i+1}.t - p_i.t|, \tag{5}$$

$$E(v) = \frac{\sum Dist(p_i, p_{i+1})}{\sum |p_{i+1}.t - p_i.t|}, \qquad p_i.l, p_{i+1}.l \in g.R \tag{6}$$

Standard deviation of speeds: $D(v)$**.** As the non-uniform driving has an important influence on the carbon emission of vehicles, we use the standard deviation to represent the discrete degree of the speeds of traveling vehicles in the $g.R$ in the past hour. We calculate this feature according to Equation 7.

$$D(v) = \sqrt{\frac{\sum [E(v) - p_i.v]^2 \cdot |p_{i+1}.t - p_i.t|}{\sum |p_{i+1}.t - p_i.t|}}, p.l \in g.R \tag{7}$$

Number of vehicles: $NumVeh$**.** We calculate the number of vehicles entering a grid by retrieving the vehicles' travel trajectories. If some points of trajectories fall into the affecting region of the grid, we believe that the vehicle has access to the grid. The same vehicle may visit a grid several times in the past hour, while the number of vehicles in the grid is only increased by one.

Travel length: Len**.** Based on the Equation 5, we sum all the distance between two consecutive points to calculate the total travel length of all trajectories in the gird g. As shown in Equation 8.

$$Len = \sum Dist(p_i, p_{i+1}), \quad p_i.l, p_{i+1}.l \in g.R \tag{8}$$

In figure 5, each row or column indicates one feature. Each plot indicates the amount of transportation carbon emission. These features are extracted from a *GPS* trajectory dataset generated by over 3,000 taxicabs in Zhuhai. As the taxicabs travel accounts for about 4.5% of the total daily travel of residents in the city [20], the dataset is big enough to represent the traffic patterns there [5].

With the increase of *NumVeh* and *NumSta*, the amount of transportation carbon emission increases significantly, as depicted in the third row and the fourth column. Vehicles are the main sources of transportation carbon emission which mainly comes from the combustion of fossil fuels. Therefore, normally the more emission sources are always producing more emissions. Just as we have known the vehicles will consume more fuel, when vehicles starts. If there are more start operations, the carbon emission should be greatly increased. When $E(v)$ is between $0km/h$ and $40km/h$, the carbon emission gradually increases and reaches the maximum value. When $E(v) > 40$, the larger $E(v)$ is, the more small amount of the carbon emission(e.g., the plot on the first column). It is surprising that not all vehicles emit less carbon emission when they are moving close to a constant speed, as showed in the first row. $D(v)$ and $E(v)$ are closely related to the analysis of transportation carbon emission. In the case of small $D(v)$, with the increase of $E(v)$ the transportation carbon emission will be reduced, i.e., in a traffic jam each vehicle has to move very slowly, the $D(v)$ is small but the carbon emission is relatively large. When $D(v)$ and $E(v)$ simultaneously increase, the carbon emission will gradually decrease. In fact, if there is no traffic jam, the speed of the vehicles on the road is varied and $D(v)$ will be maintained at a relatively large value.

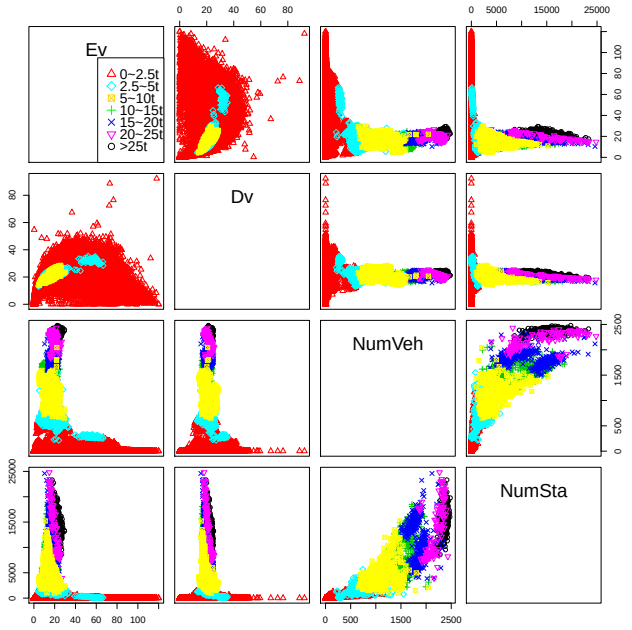

Fig. 5. Correlation matrix between traffic features and Transportation carbon emission

4.2 Mobility Features: F_{Mo}

Urban transportation is to meet the basic mobility-related needs of human. Digging out the characteristics of human mobility in different areas is necessary to the research on urban mining. Based on the characteristics of human mobility in a certain area, we can evaluate the popularity of this area. It contributes to the inference of transportation carbon emission. In our study, we select two human mobility-related features, that is the number of people arriving at (*numArr*) and leaving (*numLea*) a grid's affecting region $g.R$ in the pass hour. We extract the two features from the dataset generated by vehicles traversing the grid in the past hour. Given trajectories in the dataset, we retrieve the pickup points(p_{up}) and the corresponding drop-off points (p_{off}) falling in the grid. Obtaining these two features of each grid, we just need to traverse all trajectories once. We calculate the *numArr* and *numLea* using the Equation 9.

$$\begin{aligned} numArr &= numArr + 1, p_{up}.l \notin g_i.R, p_{off}.l \in g_i.R \\ numLea &= numLea + 1, p_{up}.l \in g_j.R, p_{off}.l \notin g_j.R \end{aligned} \tag{9}$$

where $g_i.R$ and $g_j.R$ respectively represent the affecting region of the grid g_i and the grid g_j. *numArr* indicates the number of people arriving at $g_i.R$ and *numLea* indicates the number of people leaving $g_j.R$. $p_{up}.l$ and $p_{off}.l$ respectively represent the location of the pickup points and the location of drop-off points.

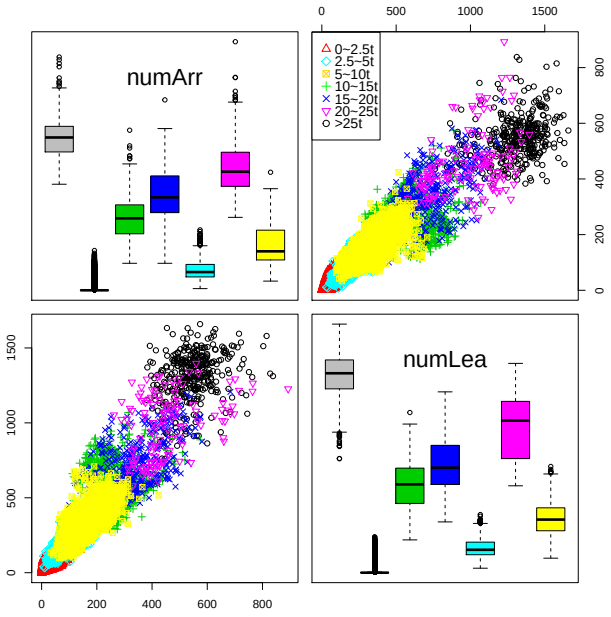

Fig. 6. Correlation matrix between mobility features and carbon emission

In figure 6, it shows the correlation matrix between transportation carbon emission and the two features, where each row and column still denotes one feature and a plot indicates the amount of transportation carbon emission of each grids in the past hour. These features are extracted from the aforementioned taxicab trajectories. As is described in the figure, with the simultaneous increase of *numArr* and *numLea*, the amount of the carbon emission has a nearly linear increase. This change is actually very reasonable, although people themselves are not the major producers of the transportation carbon emission, i.e., the prosperous region with a lot of *POI*s will attract more people from different parts of the city. The increasingly flowing of people is bound to demand a large number of vehicles. It finally will contribute to the increase of the transportation carbon emission.

4.3 POI Features: F_P

The classification and density of *POI*s tend to imply that the region's popularity and regional functions. For instance, a region with a lot of life service *POI*s has a high probability to be a residential area. Combined with the characteristics of the traffic flow, we can also learn about the frequency of communication between different functional areas. Accordingly, this information will be very helpful to infer the transportation carbon emission. We extract one feature dataset, that is the density of *POI*s for each classification in the grid. In our study, we obtain the *POI* dataset of Zhuhai by the *Auto Navi MAP*. The visual distribution of the *POI*s in the city is shown in Figure 1(b). We can clearly see that the density of *POI*s in each area is very different. As described in the Table 1, we divide the *POI* dataset into twelve classes, i.e., $\{C_1, C_2, \cdots, C_{12}\}$. The density of *POI*s for the classification C_i in the affecting region R of the grid g can be formulated by Equation 10.

$$\rho(C_i) = |\{I : I \in C_i, I.loc \in g.R\}| \tag{10}$$

where $I.loc$ is the location of the POI I.

TABLE 1
The category of *POI*s

C_1 : Vehicle Services (sales, repair)	C_7 : Hotels and Residences
C_2 : Food and Beverage	C_8 : Scenic Spots
C_3 : Shopping Services	C_9 : Culture and Eduction
C_4 : Life Services	C_{10} : Infrastructure Services
C_5 : Sports and Leisure	C_{11} : Financial Services
C_6 : Health Care	C_{12} : Companies

4.4 Road-network Features: F_{RN}

Road networks are very important for road traffic in each area and they also have great influence on the road traffic. The road networks in Zhuhai city are shown in Figure 1(b). In our study, we select the following two related features for each grid g, that is the total length of highways $f_{highway}$ and the other roads f_{road}. These two features can be formulated by the Equation 11. Figure 7 demonstrates the correlation between transportation carbon emission and this two features, utilizing the road-network dataset extracted from the *Auto Navi MAP*. The transportation carbon emission is generated by vehicles traversing the grids in the past hour. As described in the figure 7, the transportation carbon emission in each grid is strongly correlated with f_{road}. The longer f_{road}, the more transportation carbon emission. On the surface, there is a small relationship between transportation carbon emission and $f_{highway}$. However, it is clear that f_{road} and $f_{highway}$ have very different relationships with transportation carbon emission. This is also one reason why we need to separate them.

$$\begin{aligned} f_{highway} &= \sum len(r_{highway}), \qquad r_{highway} \in g.R, \\ f_{road} &= \sum len(r_{other}), \qquad r_{other} \in g.R \end{aligned} \tag{11}$$

where $len(r_{highway})$ and $len(r_{other})$ are the length of the highway $r_{highway}$ and the other road r_{other} respectively.

4.5 Meteorological Features: F_{Me}

The meteorology could potentially affect our travel plans or possibly cause us to choose short distance travel, the results will indirectly affect the amount of transportation carbon emission. Accordingly, in this section, our purpose is to identify what useful information from the meteorology can contribute to the analysis of transportation carbon emission. In the experiment, we identify two features for each grid: weather f_w and temperature f_t, which can be formulated as the Equation 12. Figure 8 illustrates the relationship between

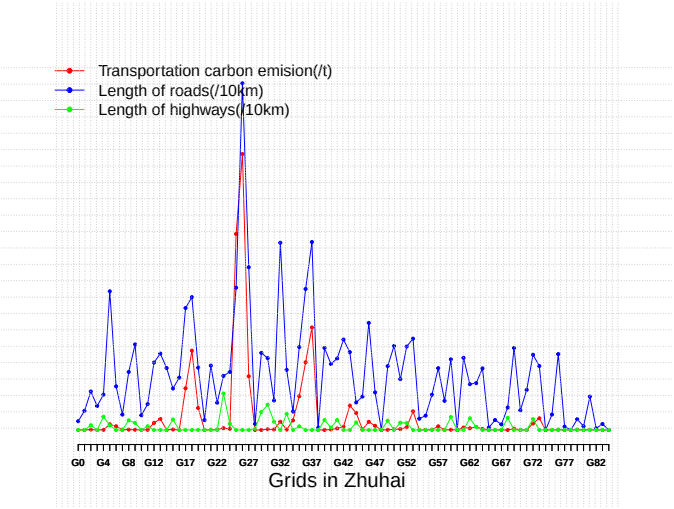

Fig. 7. The correlation between road-network features and carbon emission

the two features and the transportation carbon emission, using the meteorology data we collected from August 1st to October 31th, 2015 in Zhuhai. We mainly compare the effects of four different weather conditions on transportation carbon emission in the same region, as shown in Figure 8(a). Then we analyze the relationship between temperature and transportation carbon emission in the same region under the same weather conditions, as shown in Figure 8(b). Clearly, compared with the sunny day, transportation carbon emission under the moderate to heavy rain conditions is less. Though the effect of temperature is not obvious, the bad weather always affects people's travel. In short, these features are very discriminative in transportation carbon emission inference.

$$\begin{aligned} f_w &= weather, \qquad weather \in M \\ f_t &= temp, \qquad temp \in \mathbb{Z} \end{aligned} \tag{12}$$

where the $weather$ is the weather in the grid g. The M represents the set of weather types. The $temp$ is the temperature in the grid g.

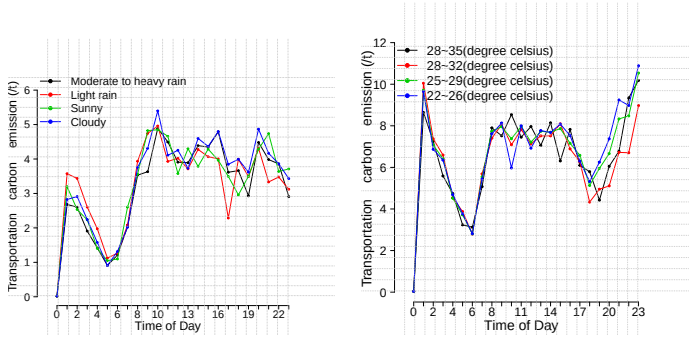

(a) Transportation carbon emission under different weature conditions in the gird $G18$.

(b) Transportation carbon emission at different temperatures under sunny day in the gird $G37$.

Fig. 8. The transportation carbon emission between difference grids

5 Learning and Inference

In this section we combine the extracted features to train our multilayer perceptron neural network and optimize the learning parameters. We aim to utilize the combination of multiple temporal and spatial features to improve the prediction. Nowadays some deep neural networks have been used in many fields such as image recognition and speech recognition, and have achieved very good results, but for our data characteristics, the performance of the deep learning algorithms is not very good. Based on the characteristics of extracted data, we propose a 3-layer perceptron neural network to infer the transportation carbon emission in the future period of time.

5.1 3-layer perceptron neural network:(3-layerPNN)

The 3-$layerPNN$ predicts the transportation carbon emission, utilizing the extracted features and the labeled data. The extracted features consist of F_T, F_{Mo}, F_P, F_{RN} and F_{Me}. The labeled data is calculated using the "top-down" approach, which is formulated in Equation 1. The main training and learning algorithm for our 3-$layerPNN$ is given in Algorithm 1. The graphical structure of our 3-$layerPNN$ is shown in Figure 9.

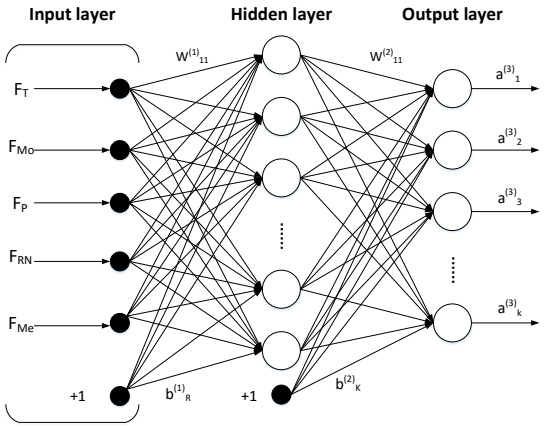

Fig. 9. The structure of the 3-layer perceptron neural network (3-$layerPNN$)

In this Figure, our 3-layer perceptron neural network consists of three layers, that is the input layer, the hidden layer and the output layer. The hidden layer contains n nodes. The output layer contains k nodes. we use the solid circles to denote the inputs of the network and utilize hollow circles to denote the multiple-inputs neurons. The solid circles labeled "+1" are used to represent the bias units and correspond to the intercept term b_i. Our neural network has parameters $(W, b) = (W^{(1)}, b^{(1)}, W^{(2)}, b^{(2)})$, where $W_{i,j}^{(l)}$ is the weight associated with the connection between unit j in layer l and unit i in layer $l+1$. $b_i^{(l)}$ denotes the bias associated with unit i in the layer $l+1$. $a_i^{(l)}$ denotes the output value of unit i in the lay l. The transfer function f of each neural in the hidden layer is the activation function $tanh$, as designed in Equation 13.

$$f(z) = tanh(z) = \frac{e^z - e^{-z}}{e^z + e^{-z}}, \tag{13}$$

Algorithm 1 The training and learning algorithm

Input: A set of features(F_T, F_{Mo}, F_P, F_{RN}, F_{Me}), the labeled data D_l for each grids, a threshold α controlling the number of epochs to run the optimizer

Output: A set of learning parameters θ of the neural networks

$3\text{-}layerPNN \leftarrow construct\ a\ three\ layers\ perceptron$
$\theta \leftarrow initialize\ the\ parameters\ \theta$
$D \leftarrow \{F_T, F_{Mo}, F_P, F_{RN}, F_{Me}\}$
$epoch \leftarrow 0$
while $epoch < \alpha$ **do**
  $epoch \leftarrow epoch + 1$
  while $True$ **do**
    $miniBatch \leftarrow read\ one\ unit\ from\ D\ and\ D_l$
    if $miniBatch\ is\ empty$ **then**
      $break$
    end if
    $put\ miniBatch\ into\ the\ Stochastic\ Gradient\ Descent\ algorithm$
    $minimize\ the\ loss\ function\ of\ 3\text{-}layerPNN\ for\ each\ sample$
    $update\ the\ parameters\ \theta\ of\ 3\text{-}layerPNN$
  end while
end while

The output layer uses the logistic regression to analyze and predict the transportation carbon emission utilizing the input data of this layer, as formulated in Equation 14. The prediction y_{pred} is the class whose probability is maximal, as formulated in Equation 15.

$$\begin{aligned} P(Y = i|x, W^{(2)}, b^{(2)}) &= softmax_i(W^{(2)}x + b^{(2)}) \\ &= \frac{e^{W_i^{(2)}x + b_i^{(2)}}}{\sum e^{W_j^{(2)}x + b_j^{(2)}}}, \end{aligned} \tag{14}$$

$$y_{pred} = argmax_i P(Y = i|x, W^{(2)}, b^{(2)}), \tag{15}$$

where Y denotes a stochastic variable. x denotes the input vector. $W^{(2)}$ is the weight matrix between units in the hidden layer and units in the output layer. $b^{(2)}$ is the bias vector associated with units in the output layer.

Formally, the computation that this 3-layer perceptron neural network represents is given by the equations as follows:

$$\begin{aligned} a^{(2)} &= f(W^{(1)}x + b^{(1)}), \\ a^{(3)} &= softmax(W^{(2)}a^{(2)} + b^{(2)}) \end{aligned} \tag{16}$$

where $a^{(2)}, a^{(3)}$ respectively denotes the output vector of the hidden layer and the output layer. $b^{(1)}$ respectively denotes the bias vector associated with units in the hidden layer. $W^{(1)}$ is the weight matrix between units in the input layer and units in the hidden layer.

To train our neural network, we use the negative log-likelihood as the loss. We use the stochastic gradient descent (*SGD*) to minimize the loss function to optimal the parameters, then update all parameters of the neural networks. The likelihood $\pounds$ and the loss ℓ are respectively defined as follow:

$$\pounds(\theta, D) = \sum_{i=0}^{|D|} log(P(Y = y^{(i)}|x^i, \theta)), \tag{17}$$

$$\ell(\theta, D) = -\pounds(\theta, D), \tag{18}$$

where θ is the set of parameters of the neural networks, $\theta = \{W^{(2)}, b^{(2)}, W^{(1)}, b^{(1)}\}$. D is the training data set.

6 Experiments

6.1 Datasets

In the experiments, we validate our prediction system using the five kinds of real world datasets in Zhuhai. We show these datasets in Table 2. Details are as follows.

Taxi trajectories: The *GPS* trajectory dataset is generated by over $3,000$ taxicabs in Zhuhai city from August 1st to October 14th, 2015. We use this dataset to calculate the F_T and F_{Mo}. Every taxicab generates a *GPS* record every 10 seconds and lasts 24 hours a day. All the taxicabs can produce about 38 million records and generate about 0.116 million kilometers in one day. According to the annual report of the traffic development in Zhuhai in 2014, the residents travel about 4.5 million times a day, and the taxicabs and small passenger cars account for about 31.8%. Each *GPS* record contains vehicle *ID*, record time, latitude, longitude, speed, direction and passenger status, etc. Utilizing map matching, we can easily count the number of taxicabs in each region and detect the condition of taxicabs on each road in the past hour. In our study, this dataset is big enough to represent the traffic patterns there. In Zheng's paper [5], he also uses the taxicab dataset to represent the traffic patterns.

Transportation carbon emission: There are two widely accepted approaches to calculate the transportation carbon emission, that is "top-down" and "bottom-up" approaches defined by *IPCC*(2006) [1]. The data required by the "bottom-up" approach is very difficult to obtain, and there is no complete data provided to this approach. However, the "top-down" approach can effectively avoid the difficulty of data acquisition. Accordingly, we use the "top-down" approach to calculate the transportation carbon emission in our experiments. The carbon emission coefficient of the taxicab is $0.5\ kg\ CO_2/km$, that is defined by the ministry of science and technology of China according to China's national conditions [21]. Additionally, the carbon emission coefficient in different countries may exist differences.

POIs: We extract the *POI* dataset of Zhuhai from the *Auto Navi MAP*. Each record of the *POI* dataset contains the *POI*'s *ID*, name, type, latitude and longitude, etc. The *POI*s are divided into multiple parts, as described in Table 1. The nember of the *POI*s in each part is shown in Figure 10. The geographical distribution of the *POI*s is described in Figure 1(b).

Road-networks: The road-network data of Zhuhai is also extracted from the *Auto Navi MAP*. Each record of this dataset contains the road-network's *ID*, road class, length and the location of the starting point, mid point and end point of the road, etc.

Meteorological data: We collect the meteorological data from a public website every day from August 1st to October 31st, 2015 in Zhuhai. Each record of this dataset consists of two messages, that is temperature and weather.

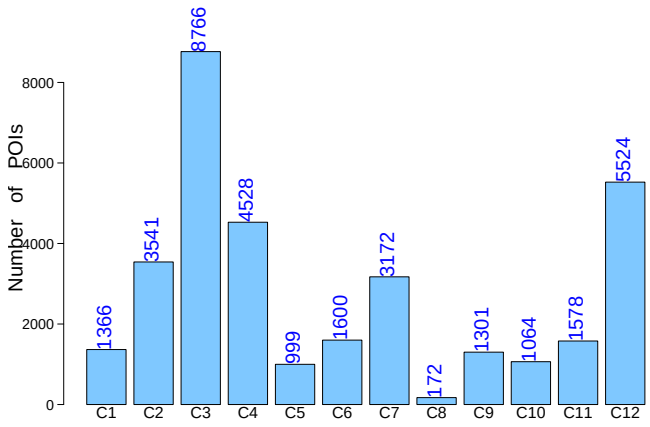

Fig. 10. Number of *POI*s in different categories

TABLE 2
Details of the datasets

Data sources		Zhuhai
taxi Trajectories	*GPS* Trajectories	2015/08/01-2015/10/14
Carbon emission	Hours	2208
	Time spans	2015/08/01-2015/10/31
Roads	Segments	30227
	Road-networks	4,420.820 km
	Highways	253.078 km
POIs	2015	38815
Meteorology	Hours	2208
	Time spans	2015/08/01-2015/10/31
Gird sizes		5×5 km

6.2 Comparison Methods

According to the characteristics of our datasets, we compare our method with three typical machine learning algorithms (Gaussian Naive Bayes, Linear Regression, Logistic Regression) and two deep learning methods (Stacked Denoising Autoencoder, Deep Belief Networks).

1) Gaussian Naive Bayes (GaussianNB): In many practical applications, the naive Bayes classifiers can be trained very efficiently in a supervised learning setting [22]. We compare with the Gauss Naive Bayes, which is shown in Equation 19 .

$$p(x = v|c) = \frac{1}{\sqrt{2\pi\sigma_c^2}} e^{-\frac{(v-\mu_c)^2}{2\sigma_c^2}}, \quad (19)$$

where x denotes a continuous attribute of the training data. v is some observation value. c denotes one class of the C.

2) Linear Regression: (LinearR) A linear regression model assumes that the relationship between the dependent variable y_i and the p-dimensional vector of regressors x_i is linear [23]. Given a dataset $\{y_i, x_{i1}, \cdots, x_{ip}\}_{i=1}^n$, the linear regression prediction model can be formulated as follows:

$$y_i = \beta_1 x_{i1} + \cdots + \beta_p x_{ip} + \varepsilon_i, \quad i = 1, 2, \cdots, n \quad (20)$$

where y_i denotes the regressand. $x_{i1}, x_{i2}, \cdots, x_{ip}$ are the input variables. $\beta_1, \beta_2, \cdots, \beta_p$ are the regression coefficients.

3) Logistic Regression (LogisticR): The Logistic regression utilize a logistic function to measure the relationship between the categorical dependent variable and one or more independent variables [24]. The logistic regression prediction model can be written as the Equation 14. In this Equation, the function $softmax$ is a standard logistic function.

4) Stacked Denoising Autoencoder (SDA): The *SDA* is a deep neural network stacked by the denoising autoencoders (*DA*) [25]. Usually, the performance of the deep learning models is better when learning high level features. In this experiment, we construct a deep learning neural network with five layers, including one input layer, three hidden layers and one output layer. These hidden layers are built by the *DA*. Each hidden layer consists of 100 neurons. The output of each hidden layer is the input to the next layer. The output layer is a logistic regression layer. The fine-tuning loop of the *SDA* is very similar to that in our 3-$layerPNN$.

5) Deep Belief Networks (DBN): The *DBN* is a deep neural network stacked by the restricted Boltzmann machines (*RBM*). The *DBN* is a graphical model which learns to extract a deep hierarchical representation of the training data [26]. In this experiment, we construct a *DBN* with four layers, including one input layer, two hidden layers and one output layer. we use the *RBM* to build the hidden layers. Each hidden layer consists of 100 neurons. The output layer is also the logistic regression layer.

6.3 Results

Evaluation on Features: We first compare and analyze the prediction performance of the single feature dataset and the fusion of multiple feature datasets. We use these different feature datasets to train the 3-$layerPNN$ model, respectively. Table 3 shows the training results of five representative combinations of the feature datasets ($F_T, F_{Mo}, F_P, F_{RN}, F_{Me}$). As described in the first three rows in the table, the prediction performance of the fusion of F_T and F_{Mo} is better than the performance of F_{Mo}, and worse than the performance of F_t. The prediction performance of the fusion of $F_T, F_{Mo}, F_P, F_{RN}, F_{Me}$ is best. The predication accuracy of the model is 90.86% utilizing the fusion of F_T, F_{Mo}, F_P, F_{RN} and F_{Me}. The results indicate that the performance of the fusion of multiple feature datasets is not always superior to the performance of the single feature dataset. However, when combined with $F_T, F_{Mo}, F_P, F_{RN}, F_{Me}$, the accuracy rate of prediction becomes better. It proves that the feature datasets we selected are very efficient. In addition, these results also suggest that feature selection is very importance for neural network training and learning.

TABLE 3
The results related to features

Features	Accuracy of the prediction
F_T	88.87 %
F_{Mo}	77.45 %
$F_T + F_{Mo}$	88.68 %
$F_P + F_{RN} + F_{Me}$	66.02 %
$F_T + F_{Mo} + F_P + F_{RN} + F_{Me}$	90.86 %

Overall Results: Leveraging the extracted five kinds of feature datasets ($F_T, F_{Mo}, F_P, F_{RN}, F_{Me}$), we train the proposed 3-$layerPNN$ and the other five aforementioned methods. The performance of these algorithms is shown in Figure 11. The predication accuracy of the 3-$layerPNN$ is 90.86%. It is clear that the 3-$layerPNN$ is more accurate than other algorithms. The results demonstrate that our method has the advantage to infer the transportation carbon emission over the other five methods. Additionally, the predication accuracy of *SDA* and *DBN* is 32.348% and 32.306% respectively. The deep learning algorithms utilize several processing layers to model high-level abstractions in data, which may lead to the distortion of training data, especially for the case of fewer feature datasets. Moreover, compared the two deep learning methods with the other methods in our experiments, it is also shown that the predication performance of the neural network with more processing layers is not always better in the transportation carbon emission areas, and the deep learning algorithm is difficult to obtain the efficient high-level abstractions based on the manually extracted feature datasets.

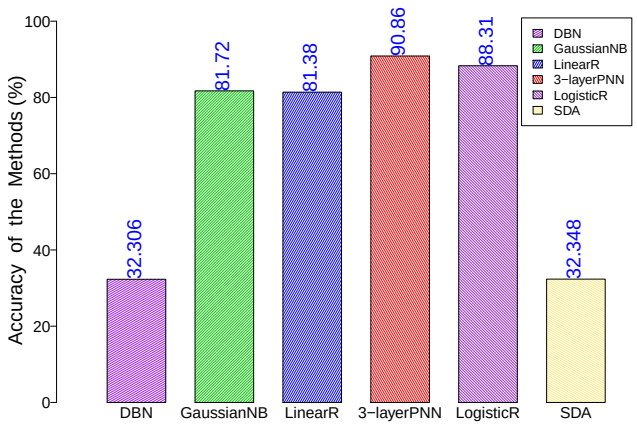

Fig. 11. Overall results of different methods

7 Conclusion

In this paper, from the perspective of big data, we predict the future transportation carbon emission based on five real world datasets (taxi trajectories, road networks, POIs, meteorological data and carbon emission data) observed in Zhuhai city. We identify five kinds of feature datasets ($F_T, F_{Mo}, F_P, F_{RN}, F_{Me}$) based on the relationship between the real world datasets and transportation carbon emission. Additionally, using the "top-down" method, we calculate the amount of transportation carbon emission as the labeled data. Accordingly, we train the proposed 3-$layerPNN$ model to infer the transportation carbon emission in the future, utilizing the extracted features and the labeled data. We evaluate our method on the basis of the spatio-temporal data obtained in the city. The results show the prediction accuracy of our method being above 90.86%, which is better than the accuracies of the other methods. Moreover, the results also demonstrate that our method is superior to the well-known machine learning algorithms (Gaussian Naive Bayes, Linear Regression, Logistic Regression) and deep learning algorithms (Stacked Denoising Autoencoder, Deep Belief Networks).

The key experiences we learn from the research lie in three aspects. Primarily, feature selection and fusion are very important for neural network training and learning. Secondly, when the extracted features are relatively few, the performance of deep learning methods may be not ideal. For instance, the prediction accuracies of the *SDA* and *DBN* algorithms are worse than the other machine learning algorithms in our experiments. Finally, the selection of the learning algorithms should be based on the unique characteristics of dataset.

In the future, we plan to extend this work in several directions. First of all, we will apply our method to more cities, in order to better characterize transportation carbon emission. Then, to reduce carbon emissions, we will consider the urban planning and vehicle scheduling to assist the decision making. Given the different amount of vehicle exhaust emissions in all regions, the management departments should optimize the traffic in different ways to cut the regional emissions. Subsequently, we would further study the data mining algorithms and theory to design more excellent algorithms for the heterogeneous urban data.

Acknowledgments

The work is supported by NSFC (No.61472149), the Fundamental Research Funds for the Central Universities (2015QN67), the National 863 Hi-Tech Research and Development Program under grant (2015AA01A203), and JSPS KAKENHI Grant Number JP16K00117, JP15K15976, KDDI Foundation.

References

[1] I. P. on Climate Change, *2006 IPCC Guidelines for National Greenhouse Gas Inventories*. Intergovernmental Panel on Climate Change, 2006.

[2] J. Davies, "Greenhouse gas emissions of the us transportation sector," *Sustainability, Energy, and Alternative Fuels*, p. 41, 2017.

[3] U. DOT, "Transportations role in reducing us greenhouse gas emissions," *US Department of Transportation, Washington, DC*, 2010.

[4] Y. Zheng, L. Capra, O. Wolfson, and H. Yang, "Urban computing: concepts, methodologies, and applications," *ACM Transactions on Intelligent Systems and Technology (TIST)*, vol. 5, no. 3, p. 38, 2014.

[5] Y. Zheng, F. Liu, and H.-P. Hsieh, "U-air: when urban air quality inference meets big data," in *Proceedings of the 19th ACM SIGKDD international conference on Knowledge discovery and data mining*. ACM, 2013, pp. 1436–1444.

[6] D. Karamshuk, A. Noulas, S. Scellato, V. Nicosia, and C. Mascolo, "Geo-spotting: mining online location-based services for optimal retail store placement," in *Proceedings of the 19th ACM SIGKDD international conference on Knowledge discovery and data mining*. ACM, 2013, pp. 793–801.

[7] J. Zhang, X. Chen, Y. Xiang, W. Zhou, and J. Wu, "Robust network traffic classification," *IEEE/ACM transactions on networking*, vol. 23, no. 4, pp. 1257–1270, 2015.

[8] D. Yang, D. Zhang, V. W. Zheng, and Z. Yu, "Modeling user activity preference by leveraging user spatial temporal characteristics in lbsns," *IEEE Transactions on Systems, Man, and Cybernetics: Systems*, vol. 45, no. 1, pp. 129–142, 2015.

[9] Z. Fan, X. Song, R. Shibasaki, and R. Adachi, "Citymomentum: an online approach for crowd behavior prediction at a citywide level," in *Proceedings of the 2015 ACM International Joint Conference on Pervasive and Ubiquitous Computing*. ACM, 2015, pp. 559–569.

[10] M. Shimosaka, K. Maeda, T. Tsukiji, and K. Tsubouchi, "Forecasting urban dynamics with mobility logs by bilinear poisson regression," in *Proceedings of the 2015 ACM International Joint Conference on Pervasive and Ubiquitous Computing*. ACM, 2015, pp. 535–546.

[11] L. DeRen, C. JianJun, and Y. Yuan, "Big data in smart cities," *SCIENCE CHINA Information Sciences*, vol. 58, no. 10, pp. 108 101–108 101, 2015.

[12] Y. Sun, H. Song, A. J. Jara, and R. Bie, "Internet of things and big data analytics for smart and connected communities," *IEEE Access*, vol. 4, pp. 766–773, 2016.

[13] J. Yang, J. Zhou, Z. Lv, W. Wei, and H. Song, "A real-time monitoring system of industry carbon monoxide based on wireless sensor networks," *Sensors*, vol. 15, no. 11, pp. 29 535–29 546, 2015.

[14] Z. Wang, H. Song, D. W. Watkins, K. G. Ong, P. Xue, Q. Yang, and X. Shi, "Cyber-physical systems for water sustainability: challenges and opportunities," *IEEE Communications Magazine*, vol. 53, no. 5, pp. 216–222, 2015.

[15] A. Abadi, T. Rajabioun, and P. A. Ioannou, "Traffic flow prediction for road transportation networks with limited traffic data," *IEEE Transactions on Intelligent Transportation Systems*, vol. 16, no. 2, pp. 653–662, 2015.

[16] Z. Wang, M. Lu, X. Yuan, J. Zhang, and H. Van De Wetering, "Visual traffic jam analysis based on trajectory data," *IEEE Transactions on Visualization and Computer Graphics*, vol. 19, no. 12, pp. 2159–2168, 2013.

[17] F. Zhang, D. Wilkie, Y. Zheng, and X. Xie, "Sensing the pulse of urban refueling behavior," in *Proceedings of the 2013 ACM international joint conference on Pervasive and ubiquitous computing*. ACM, 2013, pp. 13–22.

[18] K. Y. Chan, T. S. Dillon, and E. Chang, "An intelligent particle swarm optimization for short-term traffic flow forecasting using on-road sensor systems," *IEEE Transactions on Industrial Electronics*, vol. 60, no. 10, pp. 4714–4725, 2013.

[19] L. Chen, D. Zhang, G. Pan, X. Ma, D. Yang, K. Kushlev, W. Zhang, and S. Li, "Bike sharing station placement leveraging heterogeneous urban open data," in *Proceedings of the 2015 ACM International Joint Conference on Pervasive and Ubiquitous Computing*. ACM, 2015, pp. 571–575.

[20] Z. B. of Transportation, "Ł 2014 annual report on traffic development in zhuhai city," *Traffic and transportation*, pp. 14–15, 2015.

[21] D. of social development, M. o. s. technology, and c. technology, "People's energy saving and emission reduction practical manual," *Social Sciences Academic Press (China), Beijing*, 2007.

[22] H. Zhang, "The optimality of naive bayes," *AA*, vol. 1, no. 2, p. 3, 2004.

[23] G. A. Seber and A. J. Lee, *Linear regression analysis*. John Wiley & Sons, 2012, vol. 936.

[24] D. W. Hosmer Jr and S. Lemeshow, *Applied logistic regression*. John Wiley & Sons, 2004.

[25] P. Vincent, H. Larochelle, I. Lajoie, Y. Bengio, and P.-A. Manzagol, "Stacked denoising autoencoders: Learning useful representations in a deep network with a local denoising criterion," *Journal of Machine Learning Research*, vol. 11, no. Dec, pp. 3371–3408, 2010.

[26] G. E. Hinton, S. Osindero, and Y.-W. Teh, "A fast learning algorithm for deep belief nets," *Neural computation*, vol. 18, no. 7, pp. 1527–1554, 2006.

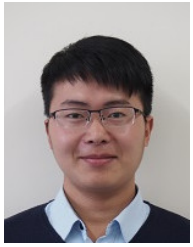

Xiangyong Lu received the B.S. degree in computer science from Henan University, Kaifeng, China, in 2015. He is currently working toward the M.S. degree in the Services Computing Technology and System Lab, Big Data Technology and System Lab, Cluster and Grid Computing Lab, School of Computer Science and Technology, Huazhong University of Science and Technology, Wuhan, 430074, China, under the guidance of Pro. Chen Yu. From April 2016 to March 2017, he is a Visiting Scholar in the Emerging Networks and Systems Lab and Wireless Networks Lab, the Department of Information and Electronic Engineering, Muroran Institute of Technology, Muroran, Hokkaido, Japan, under the guidance of Prof. Kaoru Ota. His research interests include ubiquitous computing, context-aware computing, data mining and wireless networks.

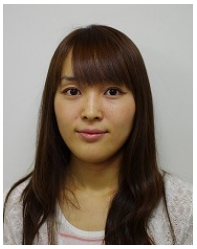

Kaoru Ota was born in Aizu Wakamatsu, Japan. She received M.S. degree in Computer Science from Oklahoma State University, USA in 2008, B.S. and Ph.D. degrees in Computer Science and Engineering from The University of Aizu, Japan in 2006, 2012, respectively. She is currently an Assistant Professor with Department of Information and Electronic Engineering, Muroran Institute of Technology, Japan. From March 2010 to March 2011, she was a visiting scholar at University of Waterloo, Canada. Also she was a Japan Society of the Promotion of Science (JSPS) research fellow with Kato-Nishiyama Lab at Graduate School of Information Sciences at Tohoku University, Japan from April 2012 to April 2013. Her research interests include Wireless Networks, Cloud Computing, and Cyber-physical Systems. Dr. Otas research results have been published in 110 research papers in international journals, conferences and books. She has received best paper awards from ICA3PP 2014, GPC 2015, and IEEE DASC 2015. She serves as an editor for IEEE Communications Letters, Peer-to-Peer Networking and Applications (Springer), Ad Hoc & Sensor Wireless Networks, International Journal of Embedded Systems (Inderscience), as well as a guest editor for IEEE Wireless Communications, IEICE Transactions on Information and Systems. She is currently a research scientist with A3 Foresight Program (2011-2016) funded by Japan Society for the Promotion of Sciences (JSPS), NSFC of China, and NRF of Korea.

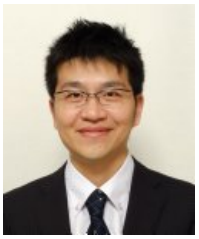

Mianxiong Dong received B.S., M.S. and Ph.D. in Computer Science and Engineering from The University of Aizu, Japan. He is currently an Associate Professor in the Department of Information and Electronic Engineering at the Muroran Institute of Technology, Japan. Prior to joining Muroran-IT, he was a Researcher at the National Institute of Information and Communications Technology (NICT), Japan. He was a JSPS Research Fellow with School of Computer Science and Engineering, The University of Aizu, Japan and was a visiting scholar with BBCR group at University of Waterloo, Canada supported by JSPS Excellent Young Researcher Overseas Visit Program from April 2010 to August 2011. Dr. Dong was selected as a Foreigner Research Fellow (a total of 3 recipients all over Japan) by NEC C&C Foundation in 2011. His research interests include Wireless Networks, Cloud Computing, and Cyber-physical Systems. His research results have been published in 130 research papers in international journals, conferences and books. He has received best paper awards from IEEE HPCC 2008, IEEE ICESS 2008, ICA3PP 2014, GPC 2015, and IEEE DASC 2015. Dr. Dong serves as an Editor for IEEE Communications Surveys and Tutorials, IEEE Network, IEEE Wireless Communications Letters, IEEE Cloud Computing, IEEE Access, and Cyber-Physical Systems (Taylor & Francis), as well as a leading guest editor for ACM Transactions on Multimedia Computing, Communications and Applications (TOMM), IEEE Transactions on Emerging Topics in Computing (TETC), IEEE Transactions on Computational Social Systems (TCSS). He has been serving as Symposium Chair of IEEE GLOBECOM 2016, IEEE ICC 2017. Dr. Dong is currently a research scientist with A3 Foresight Program (2011-2016) funded by Japan Society for the Promotion of Sciences (JSPS), NSFC of China, and NRF of Korea.

Chen Yu received the B.S. degree in mathematics and the M.S. degree in computer science from Wuhan University, Wuhan, China, in 1998 and 2002, respectively, and the Ph.D. degree in information science from Tohoku University, Sendai, Japan, in 2005.

From 2005 to 2006, he was a Japan Science and Technology Agency Postdoctoral Researcher with the Japan Advanced Institute of Science and Technology. In 2006, he was a Japan Society for the Promotion of Science Postdoctoral Fellow with the Japan Advanced Institute of Science and Technology. Since 2008, he has been with the School of Computer Science and Technology, Huazhong University of Science and Technology, Wuhan, where he is currently an Associate Professor and a Special Research Fellow, working in the areas of wireless sensor networks, ubiquitous computing, and green communications. Dr. Yu was a recipient of the Best Paper Award in the 2005 IEEE International Conference on Communication and the nominated Best Paper Award in the Proceedings of the 11th IEEE International Symposium on Distributed Simulation and Real-Time Application in 2007.

Hai Jin is a Cheung Kung Scholars Chair Professor of computer science and engineering at Huazhong University of Science and Technology (HUST) in China. Jin received his PhD in computer engineering from HUST in 1994. In 1996, he was awarded a German Academic Exchange Service fellowship to visit the Technical University of Chemnitz in Germany. Jin worked at The University of Hong Kong between 1998 and 2000, and as a visiting scholar at the University of Southern California between 1999 and 2000. He was awarded Excellent Youth Award from the National Science Foundation of China in 2001. Jin is the chief scientist of ChinaGrid, the largest grid computing project in China, and the chief scientists of National 973 Basic Research Program Project of Virtualization Technology of Computing System, and Cloud Security.

Jin is a senior member of the IEEE and a member of the ACM. He has co-authored 22 books and published over 700 research papers. His research interests include computer architecture, virtualization technology, cluster computing and cloud computing, peer-to-peer computing, network storage, and network security.